Analyst

RSC Publishing

PAPER

An aptasensor for electrochemical detection of tumor necrosis factor in human blood†

Cite this: *Analyst*, 2013, **138**, 4321

Ying Liu,* Qing Zhou and Alexander Revzin*

Received 23rd April 2013
Accepted 3rd May 2013

DOI: 10.1039/c3an00818e

www.rsc.org/analyst

Electrochemical aptasensors can detect disease markers such as cytokines to provide point-of-care diagnosis that is low-cost, rapid, specific and sensitive. Herein, we describe the development of an aptamer-based electrochemical sensor for detection and analysis of tumor necrosis factor-alpha (TNF-α) – a key inflammatory cytokine – in whole human blood. When testing spiked blood, a TNF-α detection limit of 58 pM (10 ng mL^{-1}) and a linear range of 6 nM (100 ng mL^{-1}) could be achieved. Furthermore, detection of TNF-α in mitogen stimulated whole blood was demonstrated.

Introduction

Cytokines secreted by cells play a critical role in intercellular communication that are a part of innate and adaptive immune responses.[1–4] Tumor necrosis factor-α (TNF-α) is involved in a broad range of physiological and pathological responses and is a key marker of inflammation.[5–12] For example, TNF-α is rapidly upregulated in the brain after injury and is associated with necrosis or apoptosis.[5,6] Acting as a pro-inflammatory and pro-oxidative factor, TNF-α complicates many pathologies, including atherosclerosis,[7] rheumatoid arthritis,[8] psoriasis,[9] inflammatory bowel disease,[10] Alzheimer's disease[11] and various pulmonary disorders.[12] Therefore, measuring TNF-α is important for the understanding of inflammation and discovering drugs that alleviate it.[13]

A number of traditional immunoassays have been widely employed for the detection and quantification of TNF-α, including enzyme-linked immunosorbent assay (ELISA),[14,15] radioimmunoassay,[16] fluorescence immunoassay,[17,18] and time-resolved immunofluorometric assay.[19] By and large these methods rely on antibody pairs for creation of sandwich immunoassays, requiring multiple washing steps and expensive reagents to develop the signal.

Aptamers are DNA or RNA oligonucleotides designed to bind to various biomolecules with high specificity and sensitivity. Unlike antibodies, aptamers may be easily engineered to contain affinity and signal transducing moieties into the same molecule. A number of aptasensors capable of both capturing the analyte and transducing the signal have been reported in the literature.[20–23] Detection of cell biomarkers based on aptasensors has attracted a significant amount of research interest in recent years.[24–26] Our laboratory has developed optical/electrochemical biosensors to detect cytokine molecules and to study immune cell functions. In comparison to fluorescence readout, electrochemical aptasensors may offer better signal stability, sensitivity, and ease of calibration, making them particularly appealing for applications involving complex samples.[21–23] Recently, we developed aptasensors for electrochemical sensing of IFN-γ and TNF-α and demonstrated utility of these biosensors for detecting cell-secreted cytokines.[27–29]

Building on these previous studies, we pursued the development of an aptamer-based biosensor for detection of TNF-α in complex media such as human blood. The principle of device operation, shown in Fig. 1A, is based on conformational changes of the aptamer. Binding event of the target analyte is presumed to change the distance between redox reporters and electrodes, generating detectable electrochemical signals. Importantly, aptamer electrodes can be regenerated and used multiple times (Fig. 1B).

Using such aptasensor, we were able to detect TNF-α with high sensitivity in spiked whole blood. The limit of detection (LOD) for TNF-α in whole blood was 10 ng mL^{-1} – which compares well with values of 1–20 ng mL^{-1} reported for whole blood.[30,31] Moreover, we tested the specificity, stability and reusability of this aptasensor. This paper represents one of the first demonstrations of an aptasensor being used for detection of cytokines in blood and may have significant implications for monitoring tissue injury, infectious diseases and inflammation.

Materials and methods

Materials

The following reagents were used as received: 4-(2-hydroxyethyl)-1-piperazineethanesulfonic acid (HEPES), sodium bicarbonate ($NaHCO_3$) (all reagent grade), 6-mercapto-1-hexanol (MCH), tris-(2-carboxyethyl) phosphine hydrochloride (TCEP),

Department of Biomedical Engineering, University of California, 451 Health Sciences Drive, #2519, Davis, CA, 95616, USA. E-mail: ucyliu@ucdavis.edu; arevzin@ucdavis.edu; Tel: +1-530-752-2383

† Electronic supplementary information (ESI) available. See DOI: 10.1039/c3an00818e

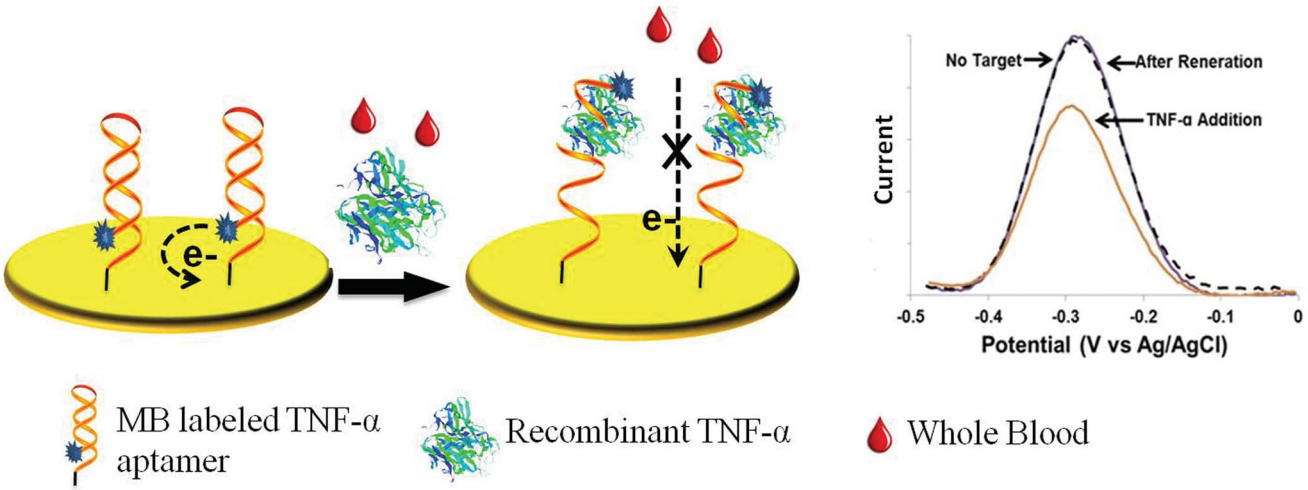

Fig. 1 (A) Schematic representation of the TNF-α aptasensor with Methylene Blue (MB) as a redox label. In the absence of target, aptamer hairpins remain folded with MB reporters in proximity to the electrode, ensuring efficient electron transfer (e^-) and a measurable faradaic current. Upon target binding, the redox tag moves further away from the electrode and the redox current decreases. (B) This RNA aptasensor can be fully regenerated using 7 M urea buffer.

urea, bovine serum albumin (BSA) (98%) (all from Sigma-Aldrich, St. Louis, MO), IgG, anti-human IgG (from BD Pharmingen), human recombinant IFN-γ, TNF-α, were purchased from R&D Systems (Minneapolis, MN), methylene blue (MB), carboxylic acid, succinimidylester (MB-NHS, Biosearch Technologies, INC, Novato, CA), and cell culture medium RPMI 1640 (1×, with L-glutamine; VWR). Medium was supplemented with penicillin/streptomycin purchased from Invitrogen. All chemicals were used without further purification.

The 28-mer TNF-α-binding aptamer sequence (IDT Technologies) was as follows: 5′-/5AmMC6/rG*rG*rA*rG*rU*rA*rU*rC*rU*rG*rA*rU*rG*rA*rC*rA*rA*rU*rU*rC*rG*rG*rA*rG*rC*rU*rC*rC/3ThioMC3-D/-3′. Phosphorothioates (or S-oligos, marked with *) were used to stabilize RNA against RNase degradation. TNF-α aptamers were modified at the 3-terminus with a C_6-disulfide [$HO(CH_2)_6$–S–S–$(CH_2)_6$–] linker and at the 5-end with an amine group for redox probe (MB) conjugation. The aptamers were dissolved in HEPES buffer (pH 7.4).

Attachment of redox labels to aptamers

The MB-tagged aptamer was prepared using a procedure similar to that described by Plaxco and co-workers.[21] Briefly, NHS-labeled MB was conjugated to the 5′-end of an amino-modified RNA aptamer through succinimide ester coupling. MB-NHS (1 μmol) was dissolved in 10 μL of DMF/40 μL of 0.5 M $NaHCO_3$, then added to 50 μL of 100 μM aptamer solution, stirred, and allowed to react for 4 h at room temperature in the dark. After reaction, the sample was filtered using a centrifugal filter (Millipore, Amicon Ultra 3K 0.5 mL) in order to purify and concentrate MB-modified aptamers. The stock aptamer solution (50 μM) was stored at −20 °C for future use.

Assembly of aptamer molecules on gold electrodes

The TNF-α sensor was fabricated using a gold working electrode ($\Phi = 5$ mm). The electrodes were cleaned in "piranha" solution consisting of a 3 : 1 ratio of 30% w/v aqueous solutions of H_2SO_4 and H_2O_2 (**Caution**: this mixture reacts violently with organic materials and must be handled with extreme care), then thoroughly washed with ethanol and DI H_2O, and dried under nitrogen. Prior to modification of the electrodes, the aptamer stock solution (0.05 mM) was reduced in 10 mM TCEP for 1 h to cleave disulfide bonds. This solution was then diluted in HEPES buffer to achieve the desired aptamer concentration (from 0.1 to 10 μM). For aptamer immobilization, the gold electrodes were kept in a solution of thiolated aptamers for 16 h in the dark at 4 °C. Following incubation, the electrodes were rinsed with copious amounts of DI water and then immersed in an aqueous solution of 3 mM 6-mercapto-1-hexanol solution (MCH) for 1 h to displace nonspecifically adsorbed aptamer molecules and to passivate the electrode surface. As a final step, the electrodes were rinsed with DI water, dried with nitrogen, and stored at 4 °C prior to use.

Surface plasmon resonance analysis of aptamer assembly and TNF-α binding

Surface plasmon resonance (SPR) experiments were performed using a two channel SPR instrument from BI (Biosensing Instrument, AZ). All experiments were performed on bare gold chips obtained from BI. Aptamers were heated to 70 °C, and cooled down to room temperature to form a hairpin structure, and then dissolved in HEPES buffer (10 mM HEPES, 150 mM NaCl). This aptamer solution was injected into the SPR device at a flow rate of 20 μL min^{-1} and was allowed to interact with the chip for 10 min. Assembly of aptamers was followed by flowing 3 mM MCH in HEPES buffer at a flow rate of 20 μL min^{-1} for 30 s. This step was needed to block the gold surface after

aptamer assembly in order to prevent nonspecific adsorption. TNF-α was dissolved in HEPES buffer and then introduced into an SPR instrument at a flow rate of 20 μL min^{-1}, remaining in contact with the SPR chip until saturation of the signal. To dissociate TNF-α and regenerate the aptamer layer, the SPR chip was washed in 7 M urea buffer. The process of surface regeneration did not compromise sensitivity of the aptamer layer and allowed us to challenge the same aptamer layer with multiple concentrations of TNF-α.

SPR sensograms were analyzed using a kinetic Langmuir 1 : 1 fitting model on Scrubber software (purchased from BI, AZ) to determine association, dissociation, and equilibrium (K_d) constants of aptamer–TNF-α binding.

Electrochemical characterization of aptasensor response to TNF-α

Electrochemical measurements were made using a CHI 842B Electrochemical Workstation (CH Instruments, Austin, TX) with a three-electrode system consisting of a Ag/AgCl (3 M KCl) reference electrode, a Pt wire counter electrode, and a gold working electrode. Electrochemical experiments were performed in 10 mM HEPES buffer using square wave voltammetry (SWV) with a 40 mV amplitude signal at a frequency of 60 Hz, over the range from −0.10 to −0.50 V *versus* Ag/AgCl references.

Electrodes were modified with aptamer molecules as described above and were placed into a custom-made Plexiglas electrochemical cell. The sensor was allowed to equilibrate for 30 min, as determined by stable faradaic current, and was then challenged with human recombinant TNF-α dissolved in HEPES buffer. Before conducting voltammetric measurements, the sensor was allowed to react with analyte for 15 min. After cytokine detection experiments, aptasensors could be regenerated by immersion in 7 M urea buffer for 1 min followed by copious rinsing with DI water. Effectiveness of the regeneration protocol was verified by SWV.

Effects of aptamer surface density on TNF-α detection in HEPES buffer and whole blood

Studies were carried out to determine how the packing density of aptamer molecules affected sensitivity and the limit of detection of the biosensor. In these SWV experiments, potential was scanned from −0.1 to −0.5 V with a step potential of 4 mV, frequency of 60 Hz, and amplitude of 40 mV. Gold electrodes were immersed in 0.1, 1.0, and 10.0 μM aptamer solution in 10 mM HEPES buffer (pH 7.4). Aptamer-coated electrodes were then incubated in 10 mM HEPES buffer (pH 7.4) for 30 min to equilibrate. The surface density of MB-labelled aptamer molecules was calculated by integrating the area under the SWV curve and converting charge to the number of surface-bound RNA molecules. Gold electrodes modified with aptamer layers of different densities were challenged with a series of concentrations of TNF-α (from 10 ng mL^{-1} to 500 ng mL^{-1}) and analyzed by SWV. The results were presented as the difference in faradaic current before and after target binding divided by the initial faradaic current. Because binding of TNF-α causes a decrease in current, the sensitivity of the biosensor was reported in terms of signal loss or suppression, with the greatest signal loss per given TNF-α concentration being the most sensitive sensor.

Electrochemical detection of TNF-α in HEPES buffer and whole blood

Calibration of the aptasensor was performed by challenging aptasensors with known concentrations of recombinant TNF-α dissolved in HEPES and whole blood. During detection of recombinant TNF-α, the electrochemical cell was placed onto a custom-made heating stage to maintain a temperature of 37 °C and to mimic conditions used in whole blood stimulation experiments.

To analyse TNF-α release from blood cells upon PMA/ionomycin stimulation, the electrochemical cell was incubated with human whole blood. The mitogenic solution consisted of PMA and ionomycin dissolved to concentrations of 50 ng mL^{-1} and 2 mM, respectively, in whole blood. SWV measurements were made every 30 min for up to 4 h. A heparinized container was used in whole blood analysis in order to prevent blood coagulation and fractionation. Pipetting blood solution thoroughly was required before each measurement to ensure the consistent signal and prevent blood fractionation.

Results and discussions

The goal of this study was to develop an electrochemical aptasensor for the detection of TNF-α in blood. Aptamer immobilization was optimized and the specificity of aptasensors for the analyte of interest was demonstrated. Significantly, detection of spiked as well as endogenous TNF-α in blood was demonstrated.

Characterization of TNF-α aptasensors

In order to arrive at the optimal TNF-α aptasensor we characterized aptamers immobilized on Au using SPR. Though the nucleic acid sequence of aptamers specific for TNF-α has been reported in the literature,[32] the position of the sensing domains on the RNA strand was not clarified. Over the course of SPR studies, ten fold higher binding was observed in aptamers immobilized *via* the 3′-end, suggesting that cytokine binding nucleotides where located closer to the 5′-end of the molecule (data not shown). Additional SPR studies described in Fig. S2† revealed equilibrium constant K_d to be 0.925 ± 0.021 nM for a naked aptamer and 0.907 ± 0.034 nM for an aptamer with MB tag at the 5′-end, suggesting that attachment of the redox label did not significantly impact cytokine–aptamer interaction. Importantly, the K_d of the TNF-α aptamer was comparable to concentrations of cytokine secreted by cells *in vitro* or observed in blood upon mitogenic stimulation.[30,31]

Additional optimization studies were carried out using square wave voltammetry (SWV). The packing density of aptamers may be an important factor contributing to biosensor response. The density of the MB-aptamer on the surface was

calculated based on the magnitude of SWV peaks.[27] The MB-aptamer surface densities were estimated to be $(1.47 \pm 0.09) \times 10^{12}$ molecules per cm^2, $(4.90 \pm 0.16) \times 10^{13}$ molecules per cm^2, and $(9.03 \pm 0.21) \times 10^{13}$ molecules per cm^2 for 0.1, 1.0, and 10.0 μM aptamer solution respectively. Increasing aptamer concentration above 10.0 μM did not result in higher surface density of the probe, suggesting steric hindrance or electrostatic repulsion between negatively charged RNA molecules at higher concentrations.[33] Additional experiments were carried out by us previously to show that aptamer-modified electrodes were responding to TNF-α but not to nonspecific proteins.[29]

Reusability and stability of TNF-α–aptasensors

One of the advantages of aptamers over antibodies is the improved chemical stability of the former that makes regeneration possible. To demonstrate this, aptamer-modified electrodes were first challenged with 100 ng mL^{-1} TNF-α, exposed to 7 M urea for 1 min and washed with DI water. Subsequently, the electrodes were tested in HEPES buffer. As shown in Fig. 2A, after 6 cycles of cytokine challenges and surface regeneration, they retained 90% of its original activity.

To be clinically useful the aptasensors need to be functional and stable in complex physiological media such as blood. The susceptibility of wild-type RNA aptamers to degradation by endogenous ribonucleases typically found in cell lysates and serum may compromise sensor performance.[18,35] To mitigate this, RNA aptamers were made more nuclease resistant by replacing nonbridging oxygens in the backbone with sulfur, producing phosphorothioates (or S-oligos).[36,37]

To verify stability, sensor performance was monitored in HEPES buffer, serum free buffer and whole blood over ten hours at 37 °C. As shown in Fig. 2B, the aptasensor was stable in HEPES or serum supplemented RPMI, however, the redox signal of the sensor decreased significantly in whole blood. This may not be an issue of stability but may be attributed to the high viscosity of blood and high cell concentration. Blood plasma/serum is about 1.8 times as viscous as water, whereas whole blood can be up to 8 times as viscous as water.[34] It is possible that the mobility of the aptamer strand with a redox reporter is inhibited somewhat in the viscous medium contributing to the decrease in current. As a possible solution we wanted to vary the surface concentration of the aptamer. It should be noted that experiments in HEPES buffer revealed intermediate aptamer concentration (1 μM) to result in the maximal signal (Fig. S2†). In contrast, a higher concentration of 10 μM was found to be optimal for blood (see Fig. S3†). Upon optimization, aptasensor stability in blood was comparable to that of HEPES or RPMI media as shown in Fig. 2B. These results demonstrate that electrodes functionalized with RNA aptamers for TNF-α were stable in blood at 37 °C over the course of 10 h. This time period is sufficient for clinical assays involving cytokine detection.

Detecting TNF-α in whole blood

In another set of experiments aptasensors were challenged with varying concentrations of TNF-α spiked into whole blood to determine the limit of detection and linear range. Fig. 3A shows SWV curves obtained in blood, with the MB reduction peak appearing at −0.25 V (*vs.* Ag/AgCl). Upon the addition of TNF-α, the peak current decreases due to analyte binding. The decrease in the signal was converted into % signal suppression and plotted *vs.* cytokine concentration to construct a calibration curve. Fig. 3B shows that optimized aptasensors were as sensitive in blood as in HEPES buffer, with a detection limit of 10 ng mL^{-1} (0.58 nM) and the linear range extending to 100 ng mL^{-1} (6 nM). The detectable TNF-α concentration is well aligned with cytokine concentrations reported in serum/blood[30,31,35] or in the proximity of activated immune cells.[36]

The ability to detect biomarkers in whole blood obviates the need for processing steps to isolate serum or plasma and makes the point-of-care application of the biosensor more likely. Aptasensors in particular hold considerable promise in the area of blood analysis[37,38] where cytokines being increasingly used for diagnosis of diseases such as TB.[39,40,41] To prove the concept of detecting endogenous TNF-α, blood was mitogenically activated with PMA/ionomycin. As shown in Fig. 4, the TNF-α aptasensor responded sensitively to its target analyte in undiluted whole blood: when 50 ng mL^{-1} PMA/2 mM ionomycin were added to blood the faradaic current decreased by ~38% after 1 h stimulation. In comparison, <5% signal suppression

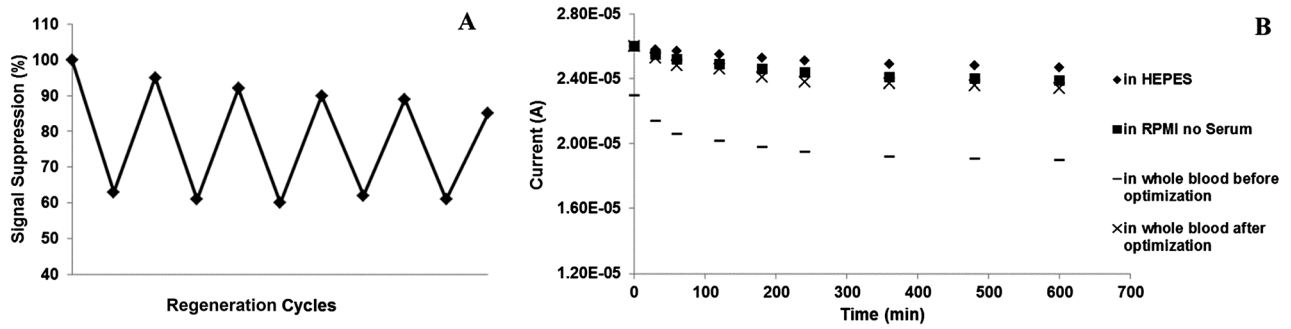

Fig. 2 (A) Reusability of the biosensor challenged with 100 ng mL^{-1} TNF-α. Cycles of cytokine challenges and surface regeneration were repeated 6 times without significant loss in the biosensor signal. Signal suppression is calculated from the values for current at SWV peaks using the formula (initial current − final current)/initial current. (B) Stability of the RNA aptasensor in HEPES buffer, serum free media and the whole blood system. It is notable that sensors remain stable in whole blood pointing to the possibility to carry out measurements in clinical samples.

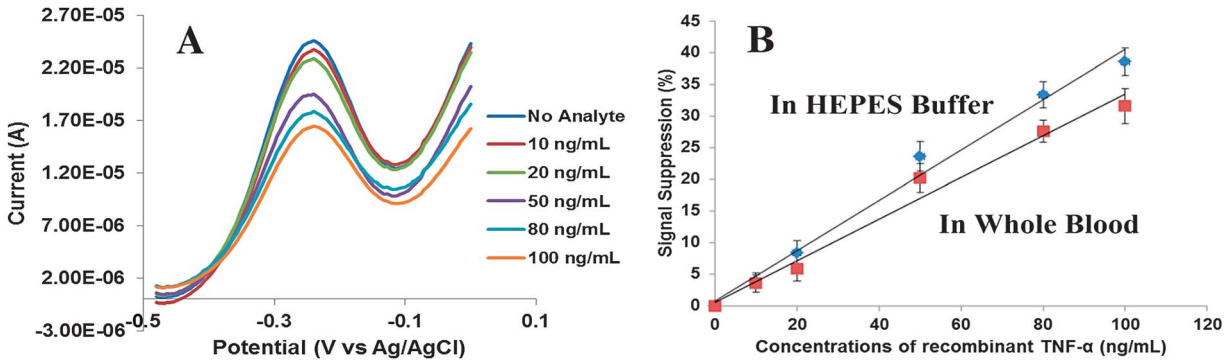

Fig. 3 Characterization of sensor responses to TNF-α. (A) SWV showed that a decrease in faradaic current was proportional to the solution concentration of TNF-α. These results were obtained using gold electrodes modified with 10 μM aptamer in whole blood. Detection limit of recombinant TNF-α is 10 ng mL^{-1} using this RNA aptasensor. (B) Calibration curves of current *vs.* TNF-α concentration for the aptasensor prepared using 1 μM aptamer concentration tested in HEPES and 10 μM aptamer concentration tested in whole blood. The calibration curves were fitted to a line with the equation of $y = 0.3806x - 0.1454$ and $R^2 = 0.9924$ in HEPES, and $y = 0.3299x + 0.5024$ and $R^2 = 0.9821$ in whole blood respectively. The data points and error bars represent average and standard deviations of measurements from three different aptamer-modified electrodes ($n = 3$).

was observed in unstimulated blood (signals were below/around the detection limit of aptasensors for negative control). After 4 h of incubation, the level of TNF-α was 2.5 fold higher compared to that of unstimulated blood at 37 °C. Our results compare well with previous reports of TNF-α production in blood after PMA stimulation.[31]

In order to further eliminate the possibility that nucleases released from cells contribute to the sensor responses we examined the performance of aptasensors after use in whole blood. Aptasensors were employed for detection of cytokine release from mitogenically activated whole blood as described above. Subsequently, blood was removed and aptasensors were regenerated by brief exposure to 7 M urea buffer. These "used" aptasensors (aptasensors have been used for detecting TNF-α from whole blood) were then challenged with varying concentrations of recombinant TNF-α and compared to pristine aptasensors that did not interact with blood and therefore could not have been exposed to endogenous nucleases. We observe no significant difference between TNF-α responses of pristine *vs.* used biosensors (see Fig. S4†), suggesting that endogenous nucleases do not interfere with sensor responses.

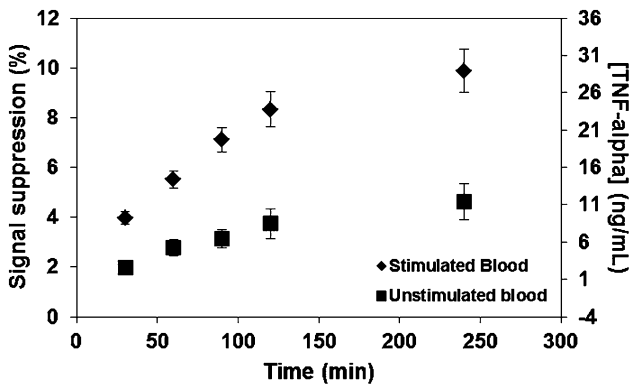

Fig. 4 Monitoring of TNF-α release from whole blood using aptamer modified electrodes. PMA/ionomycin was used as the stimulant. The calibration curve was used to convert signal suppression into TNF-α concentration (right *y*-axis).

Conclusions

We have demonstrated an electrochemical aptasensor for rapid and sensitive detection of TNF-α from whole blood. The detection limit of aptasensors for TNF-α was 10 ng mL^{-1} with the linear range extending to 100 ng mL^{-1}. To demonstrate future clinical utility of the biosensor, TNF-α was detected in mitogenically stimulated whole human blood. The sensing technology described here holds significant potential for point-of-care blood analysis, infectious diseases diagnosis, as well as injury or inflammation monitoring.

Acknowledgements

Financial support for this project was provided by the National Science Foundation (EFRI grant no. 0937997).

Notes and references

1 F. Belardelli, *APMIS*, 1995, **103**, 161–179.
2 S. Mocellin, E. Wang and F. M. Marincola, *J. Immunother.*, 2001, **24**, 392–407.
3 L. R. Watkins, S. F. Maier and L. E. Goehler, *Pain*, 1995, **63**, 289–302.
4 Z. Q. Xiang and H. C. J. Ertl, *Immunity*, 1995, **2**, 129–135.
5 F. C. Barone, B. Arvin, R. F. White, A. Miller, C. L. Webb, R. N. Willette, P. G. Lysko and G. Z. Feuerstein, *Stroke*, 1997, **28**, 1233–1244.
6 T. Liu, R. K. Clark, P. C. McDonnell, P. R. Young, R. F. White, F. C. Barone and G. Z. Feuerstein, *Stroke*, 1994, **25**, 1481–1488.
7 M. N. Sack, *Pharmacol. Ther.*, 2002, **94**, 123–135.
8 P. Sarzi-Puttini, F. Atzeni, Y. Shoenfeld and G. Ferraccioli, *Autoimmun. Rev.*, 2005, **4**, 153–161.
9 C. E. Kleyn and C. E. M. Griffiths, *Expert Opin. Biol. Ther.*, 2006, **6**, 797–805.
10 S. Danese, S. Semeraro, A. Armuzzi, A. Papa and A. Gasbarrini, *Mini-Rev. Med. Chem.*, 2006, **6**, 771–784.

11 M. Cacquevel, N. Lebeurrier, S. Cheenne and D. Vivien, *Curr. Drug Targets*, 2004, **5**, 529–534.
12 S. Mukhopadhyay, J. R. Hoidal and T. K. Mukherjee, *Respir. Res.*, 2006, **7**, 125–133.
13 M. A. Palladino, F. R. Bahjat, E. A. Theodorakis and L. L. Moldawer, *Nat. Rev. Drug Discovery*, 2003, **2**, 736–746.
14 E. F. Rossomando and L. White, *J. Periodontol.*, 1993, **64**, 445–449.
15 A. M. Yates, S. J. Elvin and D. E. Williamson, *J. Immunoassay*, 1999, **20**, 31–44.
16 A. M. Teppo and C. P. J. Maury, *Clin. Chem.*, 1987, **33**, 2024–2027.
17 S. Cesaro-Tadic, G. Dernick, D. Juncker, G. Buurman, H. Kropshofer, B. Michel, C. Fattinger and E. Delamarche, *Lab Chip*, 2004, **4**, 563–569.
18 I. Okubo, M. P. Brown, K. Chiba, R. Kasukawa and T. Nishimaki, *Mol. Biol. Rep.*, 1998, **25**, 217–224.
19 K. Zeman, J. Kantorski, E. M. Paleolog, M. Feldmann and H. Tchorzewski, *Immunol. Lett.*, 1996, **53**, 45–50.
20 Y. Xiao, A. A. Lubin, A. J. Heeger and K. W. Plaxco, *Angew. Chem., Int. Ed.*, 2005, **44**, 5456–5459.
21 Y. Xiao, R. Y. Lai and K. W. Plaxco, *Nat. Protoc.*, 2007, **2**, 2875–2880.
22 E. E. Ferapontova, E. M. Olsen and K. V. Gothelf, *J. Am. Chem. Soc.*, 2008, **130**, 4256–4258.
23 Z. W. Tang, P. Mallikaratchy, R. H. Yang, Y. M. Kim, Z. Zhu, H. Wang and W. H. Tan, *J. Am. Chem. Soc.*, 2008, **130**, 11268–11269.
24 F. Lingyan, C. Yong, R. Jinsong and Q. Xiaogang, *Biomaterials*, 2011, **32**, 2930–2937.
25 Y. Wang, Z. Li, D. Hu, C.-T. Lin, J. Li and Y. Lin, *J. Am. Chem. Soc.*, 2010, **132**, 9274–9276.
26 Z. Weian, S. Schafer, C. Jonghoon, Y. J. Yamanaka, M. L. Lombardi, S. Bose, A. L. Carlson, J. A. Phillips, T. Weisuong, I. A. Droujinine, C. H. Cui, R. K. Jain, J. Lammerding, J. C. Love, C. P. Lin, D. Sarkar, R. Karnik and J. M. Karp, *Nat. Nanotechnol.*, 2011, **6**, 524–531.
27 Y. Liu, N. Tuleouva, E. Ramanculov and A. Revzin, *Anal. Chem.*, 2010, **82**, 8131–8136.
28 Y. Liu, J. Yan, M. C. Howland, T. Kwa and A. Revzin, *Anal. Chem.*, 2011, **83**, 8286–8292.
29 Y. Liu, T. Kwa and A. Revzin, *Biomaterials*, 2012, **33**, 7347–7355.
30 L. Keski-Nisula, M. R. Hirvonen, M. Roponen, S. Heinonen and J. Pekkanen, *Eur. Cytokine Network*, 2004, **15**, 67–72.
31 K. Anttonen, A. Orpana, M. Leirisalo-Repo and H. Repo, *Ann. Rheum. Dis.*, 2006, **65**, 372–378.
32 X. Yan, X. Gao and Z. Zhang, *Genomics, Proteomics Bioinf.*, 2004, **2**, 32–42.
33 R. J. White, N. Phares, A. A. Lubin, Y. Xiao and K. W. Plaxco, *Langmuir*, 2008, **24**, 10513–10518.
34 L. R. Hirsch, J. B. Jackson, A. Lee, N. J. Halas and J. West, *Anal. Chem.*, 2003, **75**, 2377–2381.
35 R. H. See, W. W. S. Kum, A. H. Chang, S. H. Goh and A. W. Chow, *Infect. Immun.*, 1992, **60**, 2612–2618.
36 G. Stybayeva, O. Mudanyali, S. Seo, J. Silangcruz, M. Macal, E. Ramanculov, S. Dandekar, A. Erlinger, A. Ozcan and A. Revzin, *Anal. Chem.*, 2010, **82**, 3736–3744.
37 S. Zhao, W. Yang and R. Y. Lai, *Biosens. Bioelectron.*, 2011, **26**, 2442–2447.
38 A. Vallée-Bélisle, F. Ricci, T. Uzawa, F. Xia and K. W. Plaxco, *J. Am. Chem. Soc.*, 2012, **134**, 15197–15200.
39 A. Harari, V. Rozot, F. B. Enders, M. Perreau, J. M. Stalder, L. P. Nicod, M. Cavassini, T. Calandra, C. L. Blanchet, K. Jaton, M. Faouzi, C. L. Day, W. A. Hanekom, P. A. Bart and G. Pantaleo, *Nat. Med.*, 2011, **17**, 372–376.
40 R. M. D. Cunha, E. G. Kallas, D. S. Rodrigues, M. N. Burattini and R. Salomao, *Clin. Exp. Immunol.*, 2005, **140**, 491–497.
41 N. Caccamo, G. Guggino, S. A. Joosten, G. Gelsomino, P. Di Carlo, L. Titone, D. Galati, M. Bocchino, A. Matarese, A. Salerno, A. Sanduzzi, W. P. Franken, T. H. Ottenhoff and F. Dieli, *Eur. J. Immunol.*, 2010, **40**, 2211–2220.